JEM Journal of Experimental Medicine

BRIEF DEFINITIVE REPORT

Serum HBsAg clearance has minimal impact on CD8⁺ T cell responses in mouse models of HBV infection

Valeria Fumagalli[1,2], Pietro Di Lucia[1], Valentina Venzin[1,2], Elisa B. Bono[1], Robert Jordan[3], Christian R. Frey[3], William Delaney[3], Francis V. Chisari[4], Luca G. Guidotti[1,2*], and Matteo Iannacone[1,2,5*]

Antibody-mediated clearance of hepatitis B surface antigen (HBsAg) from the circulation of chronically infected patients (i.e., seroconversion) is usually associated with increased HBV-specific T cell responsiveness. However, a causative link between serum HBsAg levels and impairment of intrahepatic CD8⁺ T cells has not been established. Here we addressed this issue by using HBV replication-competent transgenic mice that are depleted of circulating HBsAg, via either spontaneous seroconversion or therapeutic monoclonal antibodies, as recipients of HBV-specific CD8⁺ T cells. Surprisingly, we found that serum HBsAg clearance has only a minimal effect on the expansion of HBV-specific naive CD8⁺ T cells undergoing intrahepatic priming. It does not alter their propensity to become dysfunctional, nor does it enhance the capacity of IL-2–based immunotherapeutic strategies to increase their antiviral function. In summary, our results reveal that circulating HBsAg clearance does not improve HBV-specific CD8⁺ T cell responses in vivo and may have important implications for the treatment of chronic HBV infection.

Introduction

Hepatitis B virus (HBV) is a noncytopathic, hepatotropic virus containing a 3.2-kb partially double-stranded DNA genome packaged together with the polymerase in viral nucleocapsids that are wrapped by envelope proteins (Guidotti and Chisari, 2006). All three in-frame envelope proteins, the large, medium, and small proteins, include the immunodominant determinant region that is detected by the diagnostic tests for hepatitis B surface antigen (HBsAg; Liaw, 2019). Besides infectious virions, HBsAg is found in the circulation in the form of noninfectious subviral spheres and filaments that are present in a 10^2–10^5-fold excess over virions, reaching exceptional quantities of up to >300 µg/ml (Kim and Tilles, 1973). The reason for evolving this extraordinary level of biosynthetic effort is not well understood, but absorption of circulating anti-HBsAg neutralizing antibodies (Abs) that would otherwise limit the spread of infectious virions within the liver is a likely explanation. The high level of circulating HBsAg has long been thought to reflect the robust transcriptional activity of an episomal, replication-competent template known as covalently closed circular DNA (Seeger and Mason, 2015). However, a recent study in chronically infected patients and chimpanzees treated with an RNA interference–based antiviral strategy has suggested that most circulating HBsAg actually derives from subgenomic, replication-incompetent HBV DNA integrants (Wooddell et al., 2017). Whatever the origin, detectable HBsAg is the serological hallmark of persistent HBV infection and, accordingly, sustained serum HBsAg loss and detection of anti-HBsAg Abs (HBsAb; seroconversion) is a widely accepted marker of therapeutic success (Fanning et al., 2019). Circulating HBsAg is thought not only to have a negative impact on antigen-specific B cell responses, but also to delete or functionally impair antigen-specific T cells (Zhu et al., 2016). This notion is supported by the observation that HBsAg seroconversion induced by nucleos(t)ide analogues is associated with an increase in the quality and vigor of HBV-specific T cell responses (Boni et al., 2012; Bazinet et al., 2020). Whether these T cell responses are actively unleashed by HBsAg loss (for instance, through cross-presentation of HBsAg–HBsAb immune complexes by professional antigen-presenting cells) or whether HBsAg loss is simply a consequence of such responses is unknown because no studies have yet systematically investigated the impact of extracellular, circulating HBsAg levels on HBV-specific CD8⁺ T cell responses at the single-cell level.

Here, we took advantage of HBV replication-competent transgenic mice that produce and secrete high levels of HBsAg

[1]Division of Immunology, Transplantation and Infectious Diseases, Istituto di Ricovero e Cura a Carattere Scientifico (IRCCS) San Raffaele Scientific Institute, Milan, Italy; [2]Vita-Salute San Raffaele University, Milan, Italy; [3]Gilead Sciences, Foster City, CA; [4]Deparment of Immunology and Microbial Sciences, The Scripps Research Institute, La Jolla, CA; [5]Experimental Imaging Center, Istituto di Ricovero e Cura a Carattere Scientifico (IRCCS) San Raffaele Scientific Institute, Milan, Italy.

*L.G. Guidotti and M. Iannacone contributed equally to this paper; Correspondence to Matteo Iannacone: iannacone.matteo@hsr.it; Luca G. Guidotti: guidotti.luca@hsr.it.

from integrated viral DNA to show that Ab-mediated clearance of circulating HBsAg has minimal impact on the expansion of HBV-specific CD8⁺ T cells. It does not alter their differentiation, nor does it enhance their functional restoration by immunotherapeutic strategies.

Results and discussion

A fraction of HBV replication-competent transgenic mice spontaneously clear serum HBsAg

We began this study by longitudinally measuring HBsAg concentrations in the serum of HBV replication-competent transgenic (HBV Tg) mice (Guidotti et al., 1995) that are profoundly tolerant to HBV-encoded antigens at the T cell level (Shimizu et al., 1998) and maintain high levels of hepatocellular HBV gene expression and replication (displaying viremias of ∼10^7–10^8 viral genomes per milliliter) without developing signs of spontaneous liver immunopathology (Guidotti et al., 1995). Surprisingly, we found that, beginning at around 7 wk of age, serum HBsAg levels in some HBV Tg mice gradually decrease over time, so that, at the end of the >20-wk observation period, ∼60% of HBV Tg mice on a C57BL/6 background and ∼70% of HBV Tg mice on a C57BL/6 × Balb/c (H-2^{bxd}) F1 hybrid background showed undetectable serum HBsAg (Fig. 1, A and B). Interestingly, there was no difference in the early (<7 wk) concentrations of serum HBsAg between mice that eventually lost serum HBsAg and mice that did not (Fig. 1 B). Also, serum HBsAg concentrations in mice that did not become HBsAg-negative remained unchanged for the entire observation period, thus allowing us to stratify mice into two distinct groups (referred to hereafter as HBsAg⁺ and HBsAg⁻ mice; Fig. 1 B). Moreover, we found no correlation between early serum hepatitis e antigen (HBeAg) concentrations (an indirect marker of hepatic HBV gene expression), serum transaminases, or viremia and subsequent serum HBsAg loss (Fig. 1 C and Fig. S1, A and B); conversely, the absence of serum HBsAg (even for a period longer than 10 wk) had no effect on serum HBeAg levels (Fig. 1 C). Serum HBsAg clearance associated with a significant reduction in viremia and serum HBV RNA (Fig. 1, D and E; and Fig. S1 B). The hepatic content of HBV transcripts and HBV replicative intermediates as well as the lobular distribution of HBV core antigen (HBcAg) appeared comparable in HBsAg⁺ and HBsAg⁻ mice (Fig. S1, C and D; and Fig. 1 F), indicating that clearance of serum HBsAg is not due to a decreased expression of HBV gene products in the liver. Hepatocellular retention is also not likely the cause of HBsAg clearance from the serum, as this rapidly secreted Ag remained undetectable in the liver of both HBsAg⁺ and HBsAg⁻ mice (Fig. S1 E). Finally, we saw no evidence of spontaneous immunopathology in HBsAg⁻ mice, as assessed by serum transaminases and intrahepatic leukocyte recruitment (Fig. 1, G and H; and Fig. S1 A), suggesting that HBsAg clearance does not cause overt reactivation of the HBV-specific tolerant T cells present in HBV Tg mice. Together, these results show that the majority of HBV Tg mice undergo spontaneous serum HBsAg loss and raise the question of what the underlying mechanism is.

Spontaneous HBsAg loss in HBV Tg mice is due to HBsAb

We reasoned that the spontaneous serum HBsAg loss observed in HBV Tg mice might be due to the production of HBsAb. Indeed, HBsAb were detected in the plasma of >50% of HBsAg⁻ mice beginning at 13 wk of age, while they were always undetectable in HBsAg⁺ mice (Fig. 2, A and B). Note that the slight delay between HBsAg loss and HBsAb detection (Fig. 1 B and Fig. 2 A), as well as the observation that not all HBsAg⁻ mice showed detectable level of HBsAb in their sera (Fig. 2 B), might be due to the presence of HBsAg–HBsAb complexes that cannot be picked up by our ELISA-based detection assay. The observation that a PCR-based assay still detects serum HBV DNA and RNA in HBsAg⁻ mice (albeit at very low levels; Fig. 1, D and E) further supports the presence of circulating immune complexes in these animals. To assess whether such HBsAg loss observed in HBsAg⁻ mice is indeed due to HBsAb, we crossed HBV Tg mice to D_HLMP2a mice that lack both surface and circulating immunoglobulins (Casola et al., 2004). All of the resulting Ab-deficient HBV Tg × D_HLMP2a mice showed detectable levels of circulating HBsAg (Fig. 2, C and D). HBV Tg mice × D_HLMP2a mice showed serum HBsAg concentrations, serum HBeAg concentrations at weaning and throughout the observation period, as well as serum HBV DNA levels, that are comparable to those of Ab-competent HBV Tg mice (Fig. 2, D–F; and data not shown). Finally, HBV Tg mice × D_HLMP2a mice showed no evidence of liver immunopathology (Fig. 2, G and H; and data not shown) and had hepatic HBcAg amount and staining pattern that are comparable to those of Ab-competent HBV Tg mice (Fig. 2 I). Together, the results indicate that the spontaneous HBsAg loss observed in HBV Tg mice is indeed due to Ab-mediated clearance (i.e., seroconversion). While the reason behind the seroconversion in a significant fraction of HBV Tg mice is unclear and might be different from that occurring in patients, the results are in line with the notion that most chronically infected patients keep producing low levels of HBsAbs in spite of retaining dysfunctional T cell responses (de Niet et al., 2014). Of note, these Abs are not quantitatively sufficient to appreciably reduce the large excess of serum HBsAg and circulate as immune complexes that cannot be detected by currently available diagnostic tests (de Niet et al., 2014).

Circulating HBsAg has no impact on the capacity of HBV-specific effector CD8⁺ T cells to induce liver immunopathology

We next took advantage of HBV Tg mice undergoing spontaneous seroconversion to study the role of circulating HBsAg in modulating HBV-specific CD8⁺ T cell responses. First, we adoptively transferred into HBsAg⁺ and HBsAg⁻ HBV Tg mice HBV envelope-specific CD8⁺ TCR transgenic T cells that had been differentiated in vitro into effector cells (Isogawa et al., 2013; Guidotti et al., 2015; HBV envelope-specific T cells [Env28 T_E]; Fig. 3 A). Serum HBsAg concentrations in recipient mice before the adoptive transfer of HBV-specific CD8 T_E are shown in Fig. 3 B. The presence of circulating HBsAg had no impact on either the magnitude or the duration of T cell–induced liver disease, as assessed by serum transaminase elevation (Fig. 3 C). In line with this, the number and the phenotype of Env28 T_E recovered from the liver was equivalent in HBsAg⁺ and HBsAg⁻ HBV Tg mice (Fig. 3, D–F; and Fig. S2 A). Finally, in keeping with the known antiviral activity of HBV-specific

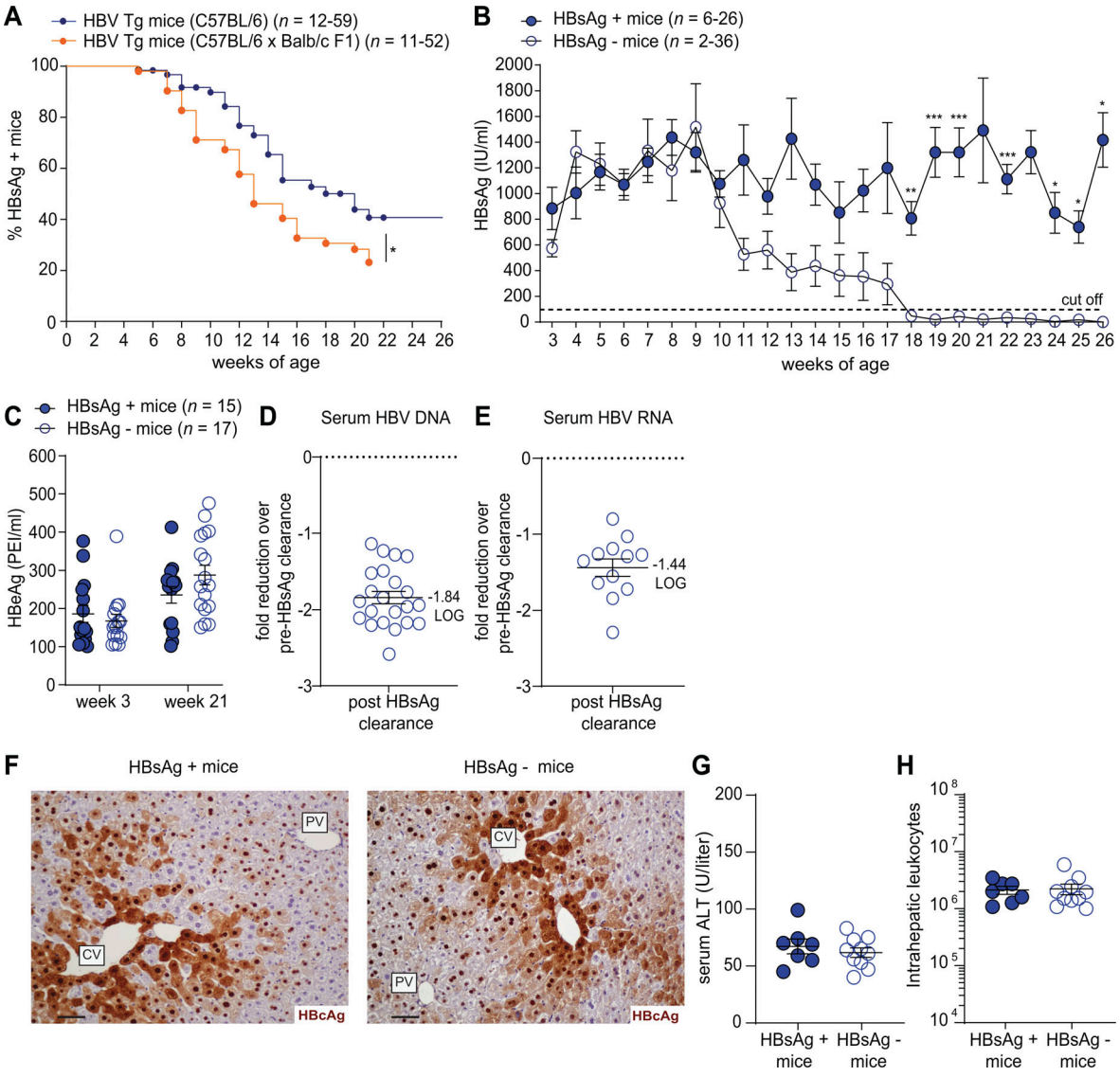

Figure 1. **A fraction of HBV replication-competent transgenic mice spontaneously clear serum HBsAg. (A)** Percentage of mice with detectable serum HBsAg (HBsAg$^+$ mice) over time in HBV Tg mice on a C57BL/6 background (blue, *n* = 12–59) and HBV Tg mice on a C57BL/6 × Balb/c F1 hybrid background (orange, *n* = 11–52). **(B)** Serum HBsAg concentrations (IU/ml) of HBV Tg mice monitored weekly by ELISA assay (cutoff set at 100 IU/ml). Solid symbols: HBsAg$^+$ mice (*n* = 6–26); empty symbols: HBsAg$^-$ mice (*n* = 2–36). **(C)** Serum HBeAg concentrations (PEI/ml) detected by ELISA assay in HBsAg$^+$ (solid symbols, *n* = 15) or HBsAg$^-$ (empty symbols, *n* = 17) mice at 3 and 21 wk of age. **(D)** HBV DNA quantification in serum of HBV Tg mice after HBsAg clearance (*n* = 22). Values expressed as fold reduction over pre-HBsAg clearance. **(E)** HBV RNA quantification in serum of HBV Tg mice after HBsAg clearance (*n* = 12). Values expressed as fold reduction over pre-HBsAg clearance. **(F)** Representative immunohistochemical micrographs of liver sections from HBsAg$^+$ (left) and HBsAg$^-$ (right) mice. HBcAg expression is shown in brown. Scale bars, 20 µm. CV, central vein; PV, portal vein. **(G and H)** Serum transaminase activity (ALT, U/liter; G) and absolute number of intrahepatic leukocytes (H) in HBsAg$^+$ (solid symbols, *n* = 7) and HBsAg$^-$ (empty symbols, *n* = 10) HBV Tg mice at 20 wk of age. Data are expressed as mean ± SEM. Results are representative of at least three independent experiments. *, P < 0.05, **, P < 0.01, ***, P < 0.001; log-rank (Mantel–Cox) test (A), two-way ANOVA followed by Sidak's multiple comparison test (B), or Mann–Whitney *U* test (C, G, and H). Comparisons are not statistically significant unless indicated.

effector CD8$^+$ T cells (Guidotti et al., 1996), hepatic HBV replication was suppressed and cytoplasmic HBcAg became undetectable in the vast majority of hepatocytes in both groups of mice (Fig. S2 B and Fig. 3 G). Similar results were obtained when HBV core-specific effector CD8$^+$ T cells (Cor93 T_E) were used in place of Env28 T_E (Fig. S2, C–J). Thus, the capacity of HBV-specific effector CD8$^+$ T cells to induce transient liver immunopathology is independent of circulating extracellular HBsAg.

Circulating HBsAg has minimal effects on the expansion of HBV-specific naive CD8$^+$ T cells undergoing hepatocellular antigen recognition, and it does not alter their differentiation into dysfunctional cells

We next investigated the influence of circulating, extracellular HBsAg on the de novo priming of naive HBV-specific CD8$^+$ T cells upon adoptive transfer into HBV Tg mice. Previous studies have shown that, upon transfer into HBV Tg mice, HBV-specific naive CD8$^+$ TCR transgenic T cells undergo

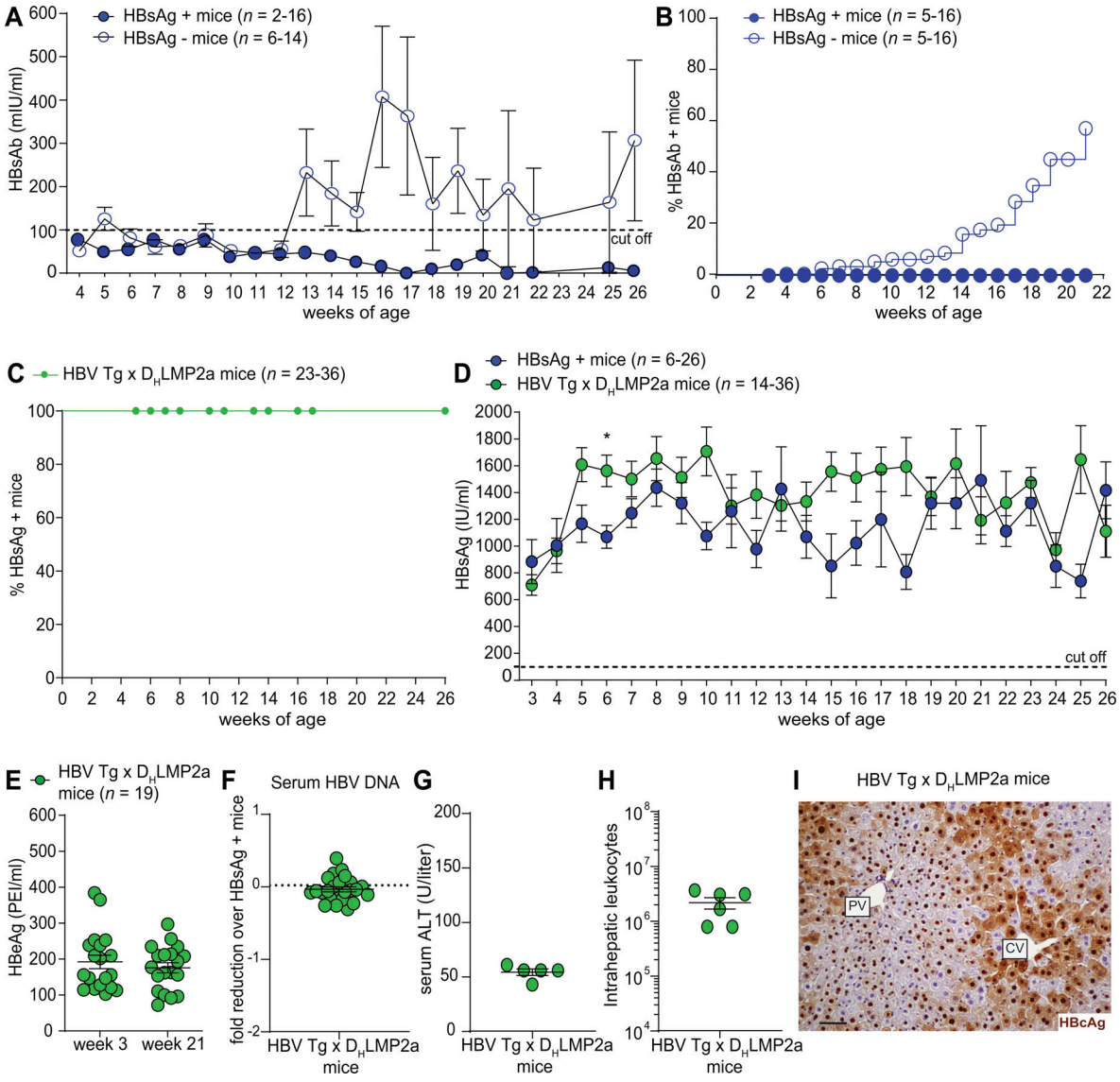

Figure 2. **Spontaneous HBsAg loss in HBV Tg mice is due to HBsAb. (A)** Serum HBsAb titers (HBsAb, mIU/ml) in HBsAg$^+$ (solid symbol, n = 2–16) and HBsAg$^-$ (empty symbols, n = 6–14) HBV Tg mice monitored weekly by ELISA assay (cutoff set at 100 mIU/ml). **(B)** Percentage of HBsAg$^+$ (solid symbols, n = 5–16) and HBsAg$^-$ (empty symbols, n = 5–16) HBV Tg mice with detectable serum HBsAb (HBsAb$^+$ mice) over time. **(C)** Percentage of HBV Tg × D_HLMP2a mice (n = 23–36) with detectable serum HBsAg (HBsAg$^+$ mice) over time. **(D)** Serum HBsAg concentrations (IU/ml) of Ab-competent HBsAg$^+$ HBV Tg mice (blue, n = 6–26) and HBV Tg × D_HLMP2a mice (green, n = 14–36) monitored weekly by ELISA assay (cutoff set at 100 IU/ml). **(E)** Serum HBeAg concentrations (PEI/ml) measured by ELISA assay in HBV Tg × D_HLMP2a mice (n = 19) at 3 and 21 wk of age. **(F)** Serum HBV DNA quantification in HBV Tg × D_HLMP2a mice (n = 24). Values expressed as fold reduction over Ab-competent HBsAg$^+$ HBV Tg mice. **(G and H)** Serum transaminase activity (ALT, U/liter; G) and absolute number of intrahepatic leukocytes (H) in HBV Tg × D_HLMP2a mice (n = 5 or 6) at 12 wk of age. **(I)** Representative immunohistochemical micrographs of liver sections from HBV Tg × D_HLMP2a mice. HBcAg expression is shown in brown. Scale bars, 20 µm. CV, central vein; PV, portal vein. Data are expressed as mean ± SEM. Results are representative of at least three independent experiments. *, P < 0.05; log-rank (Mantel–Cox) test (B and C), two-way ANOVA followed by Sidak's multiple comparison test (A–D). Comparisons are not statistically significant unless indicated.

hepatocellular antigen recognition, which leads to local activation, vigorous proliferation, but failure to develop antiviral effector functions (Isogawa et al., 2013; Bénéchet et al., 2019). Thus, to address the role of HBsAg on the intrahepatic priming of naive CD8$^+$ T cells, Cor93-specific naive CD8$^+$ TCR transgenic T cells (Cor93 T_N) were adoptively transferred into HBsAg$^+$ and HBsAg$^-$ HBV Tg mice (Fig. 4 A). Serum HBsAg concentrations in recipient mice before the adoptive transfer of Cor93 T_N are shown in Fig. 4 B. When we looked at the number of Cor93 T cells that we could recover from the liver 5 d after adoptive transfer, we noticed a minimal, although statistically significant, increase in intrahepatic Cor93 T cell numbers in the HBsAg$^-$ HBV Tg mice (Fig. 4 C). The reason for this minor difference is unclear, but the absence of circulating HBsAg had absolutely no impact on the activation state (Fig. 4, D–G) or the phenotype (Fig. S3 A) of the intrahepatic naive HBcAg-specific CD8$^+$ T cells following antigen recognition in the liver. These dysfunctional cells accumulated in the characteristic periportal clusters

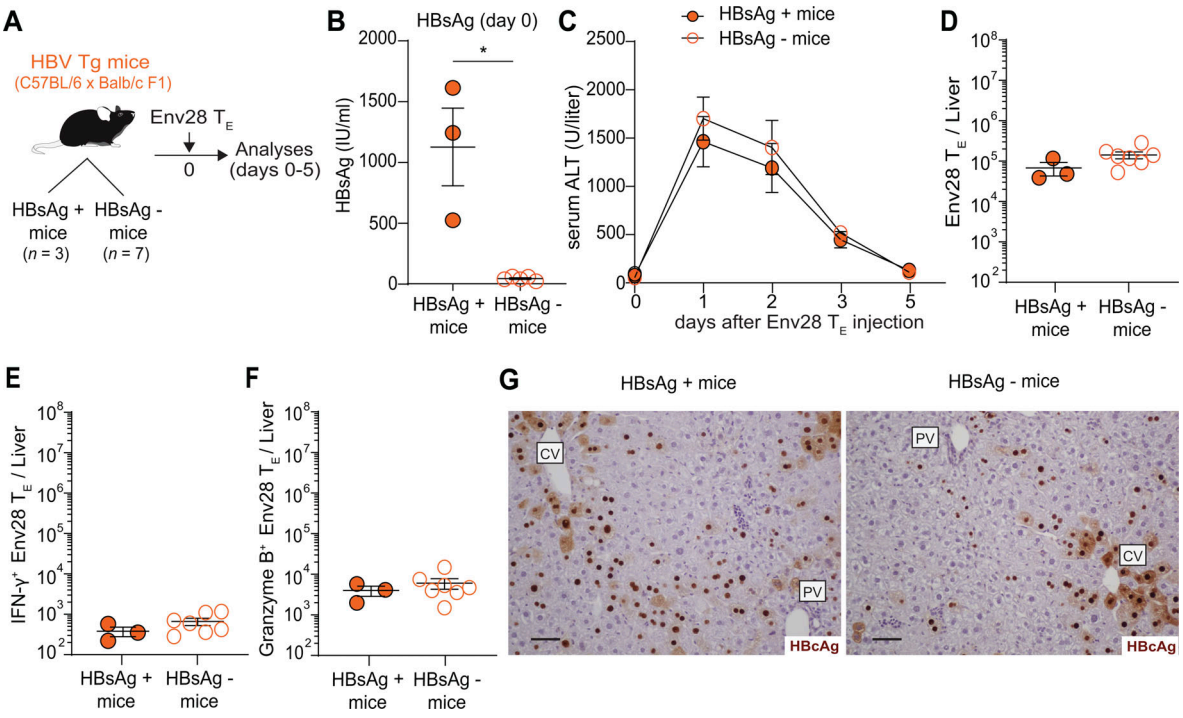

Figure 3. **Circulating HBsAg has no impact on the capacity of HBV-specific effector CD8⁺ T cells to induce liver immunopathology. (A)** Schematic representation of the experimental setup (mouse drawings were adapted from Bénéchet et al., 2019). HBsAg⁺ (solid symbols, *n* = 3) and HBsAg⁻ (empty symbols, *n* = 7) HBV Tg mice (on a C57BL/6 × Balb/c F1 hybrid background) received 10^7 HBsAg-specific effector CD8⁺ T cells (Env28 T_E). Livers were collected and analyzed 5 d after Env28 T_E transfer. Serum was collected immediately before and 1, 2, 3, and 5 d after Env28 T_E transfer. **(B)** Serum HBsAg concentrations (IU/ml) in HBsAg⁺ and HBsAg⁻ HBV Tg mice before Env28 T_E injection. **(C)** Serum transaminase activity (ALT, U/liter) in HBsAg⁺ and HBsAg⁻ HBV Tg mice after Env28 T_E injection. **(D–F)** Absolute number of (D) total Env28 T_E and absolute number of (E) IFN-γ– and (F) Granzyme B–producing Env28 T_E cells in the livers of HBsAg⁺ and HBsAg⁻ HBV Tg mice 5 d after Env28 T_E injection. **(G)** Representative immunohistochemical micrographs of liver sections from HBsAg⁺ (left) and HBsAg⁻ (right) HBV Tg mice 5 d after Env28 T_E transfer. HBcAg expression is shown in brown. Scale bars, 20 µm. CV, central vein; PV, portal vein. Data are expressed as mean ± SEM. Results are representative of two independent experiments. *, P < 0.05; Mann–Whitney *U* test (B and D–F), two-way ANOVA followed by Sidak's multiple comparison test (C). Comparisons are not statistically significant unless indicated.

(Bénéchet et al., 2019) and did not have any effect on hepatic HBcAg expression, regardless of serum HBsAg concentrations (Fig. 4 H). Similar results were obtained when HBV envelope-specific naive CD8⁺ T cells (Env28 T_N) were used in place of Cor93 T_N (Fig. S3, B–I).

To confirm these findings in a potential therapeutic setting, we treated HBsAg⁺ HBV Tg mice with an anti-HBsAg monoclonal Ab that completely depletes circulating extracellular HBsAg (Fig. 4, I and J). 15 d after the first HBsAb (or isotype control) injection, we adoptively transferred both Cor93 and Env28 naive CD8⁺ T cells and measured their intrahepatic number and function 5 d later. Consistent with the data reported in Fig. 4, A–H, HBsAg clearance caused a minimal increase in intrahepatic HBV-specific CD8⁺ T cell number, but it had no impact on their functional response or phenotypic differentiation upon recognition of their cognate antigens when presented intrahepatically by the hepatocytes (Fig. 4, K–O). Together, the results indicate that Ab-mediated clearance of HBsAg has minimal impact on the expansion of HBV-specific CD8⁺ T cells undergoing intrahepatic priming, and it does not alter their propensity to evolve into dysfunctional cells lacking antiviral effector functions as a consequence of the inhibitory effects of hepatocellular antigen presentation (Isogawa et al., 2013; Bénéchet et al., 2019).

Circulating HBsAg does not affect the functional improvement of intrahepatically primed CD8⁺ T cells by IL-2–based immunotherapeutic strategies

We have recently shown that IL-2–based immunotherapeutic strategies can prevent or reverse the dysfunctional CD8⁺ T cell response to intrahepatic antigen presentation (Bénéchet et al., 2019). We therefore set out to address whether the therapeutic effect of IL-2–based treatment was affected by circulating, extracellular HBsAg. To this end, we injected HBV Tg × D_HLMP2a mice with HBsAb (or isotype control) before the adoptive transfer of Cor93 T_N (Fig. 5 A). Selected mice received IL-2/anti–IL-2 immune complexes (IL-2c; Boyman et al., 2006; Bénéchet et al., 2019) 1 d after T cell transfer (Fig. 5 A). Serum HBsAg concentrations in recipient mice before the adoptive transfer of Cor93 T_N are shown in Fig. 5 B. Of note, HBsAg clearance did not alter the capacity of IL-2c to increase Cor93 T cell expansion and intraparenchymal accumulation, and to induce their cytolytic, IFN-γ–producing and antiviral functions (Fig. 5, C–G). Thus, exposure to circulating HBsAg does not affect the functional improvement of intrahepatically primed CD8⁺ T cells by IL-2–based immunotherapeutic strategies.

Together, the data reported here indicate that Ab-mediated clearance of circulating HBsAg has minimal effect on the expansion of HBV-specific CD8⁺ T cells. It does not affect their

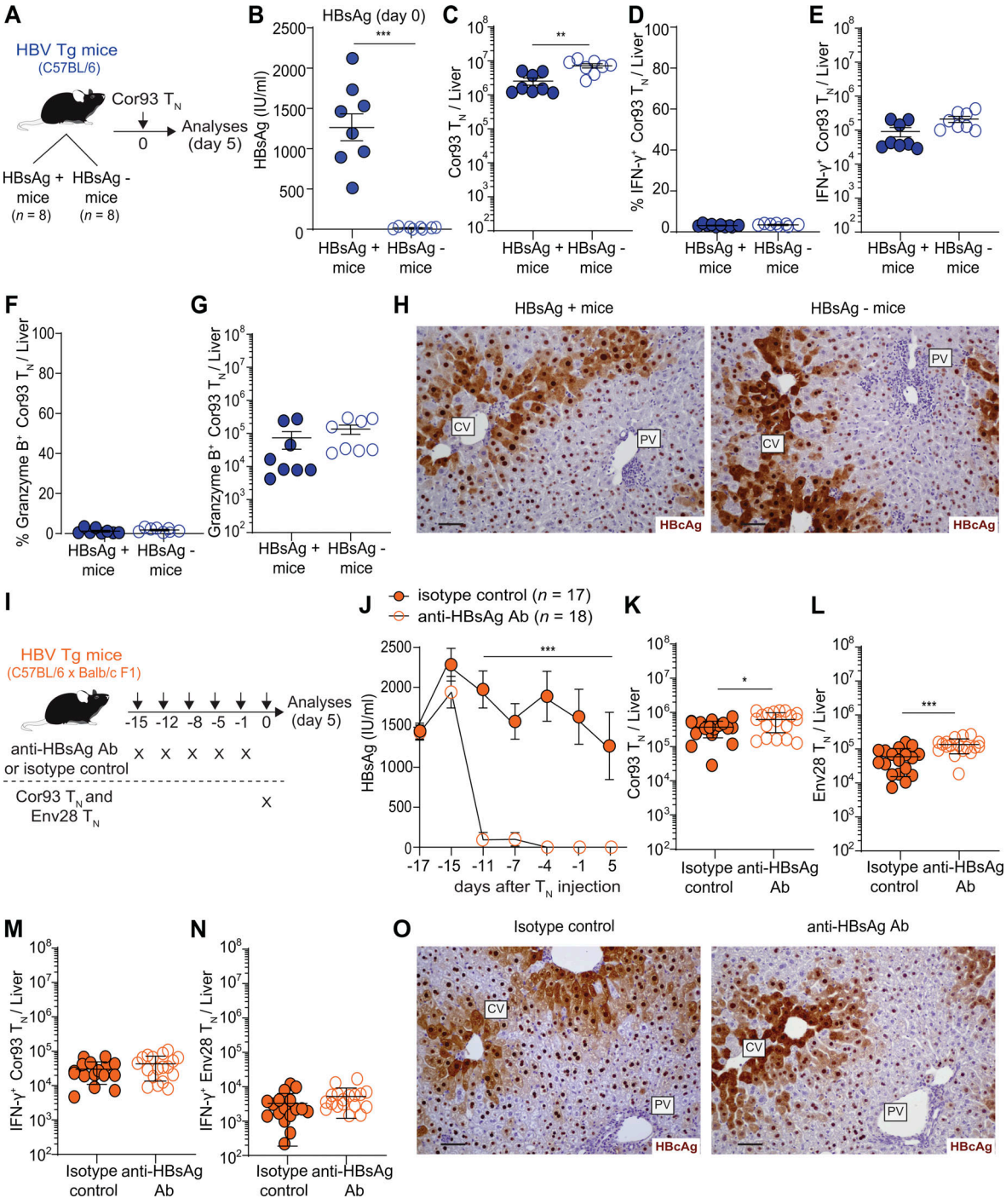

Figure 4. **Circulating HBsAg has minimal effects on the expansion of HBV-specific naive CD8⁺ T cells undergoing hepatocellular antigen recognition, and it does not alter their differentiation into dysfunctional cells. (A)** Schematic representation of the experimental setup (mouse drawings were adapted from Bénéchet et al., 2019). HBsAg⁺ (solid symbols, *n* = 8) and HBsAg⁻ (empty symbols, *n* = 8) HBV Tg mice received 2.5 × 10^6 HBcAg-specific naive CD8⁺ T cells (Cor93 T_N). Livers were collected and analyzed 5 d after Cor93 T_N transfer. Serum was collected immediately before and 5 d after Cor93 T_N transfer. **(B)** HBsAg concentrations (IU/ml) in the serum of HBsAg⁺ and HBsAg⁻ HBV Tg mice before Cor93 T_N injection. **(C)** Absolute number of total Cor93 T_N in the livers of HBsAg⁺ and HBsAg⁻ HBV Tg mice 5 d after Cor93 T_N injection. **(D–G)** Percentage (D and F) and absolute number (E and G) of IFN-γ⁺ (D and E) and Granzyme B⁺ (F and G) Cor93 T_N cells in the livers of HBsAg⁺ and HBsAg⁻ HBV Tg mice 5 d after Cor93 T_N injection. **(H)** Representative immunohistochemical micrographs of liver sections from HBsAg⁺ (left) and HBsAg⁻ (right) HBV Tg mice 5 d after Cor93 T_N injection. HBcAg expression is shown in brown. Scale bars, 20 µm. CV, central vein; PV, portal vein. **(I)** Schematic representation of the experimental setup (mouse drawings were adapted from Bénéchet et al., 2019). HBV Tg mice (on a C57BL/6 × Balb/c F1 hybrid background) were treated with HBsAb (empty symbols, *n* = 18) or isotype control (solid symbols, *n* = 17) 15, 12, 8, 5, and 1 d before receiving 2.5 × 10^6 HBcAg-specific naive CD8⁺ T cells (Cor93 T_N) and 2.5 × 10^6 HBsAg-specific naive CD8⁺ T cells (Env28 T_N). Livers were collected and analyzed 5 d after T cell transfer. Serum was collected during the Ab treatment and 5 d after T cell transfer. **(J)** Serum HBsAg concentrations (IU/ml) in mice injected with HBsAb or isotype control. **(K and M)** Absolute number of total Cor93 T cells (K) and absolute number of IFN-γ–producing Cor93 T cells (M) in the livers of mice injected with HBsAb or isotype control and sacrificed 5 d after T cell transfer. **(L and N)** Absolute number of total Env28 T cells (L) and absolute

number of IFN-γ–producing Env28 T cells (N) in the livers of mice injected with HBsAb or isotype control and sacrificed 5 d after T cell transfer. **(O)** Representative immunohistochemical micrographs of liver sections from mice injected with isotype control (left) or HBsAb (right) and sacrificed 5 d after T cell transfer. HBcAg expression is shown in brown. Scale bars, 20 µm. CV, central vein; PV, portal vein. Data are expressed as mean ± SEM. Results are representative of two (A–H) and four (I–O) independent experiments. *, P < 0.05, **, P < 0.01, ***, P < 0.001; Mann-Whitney *U* test (B–G and K–N); two-way ANOVA followed by Sidak's multiple comparison test (J). Comparisons are not statistically significant unless indicated.

differentiation, nor does it interfere with their functional improvement by immunotherapeutic strategies. These results, obtained in immunocompetent mouse models of HBV pathogenesis in which T cell tolerance and production of high levels of HBsAg from integrated viral DNA mimic some aspects of chronic HBV infection in humans, seems at a first glance to be at odds with the observation that HBsAg seroconversion in patients under nucleos(t)ide analogue therapy is often associated with an increase in the quality and vigor of HBV-specific T cell responses (Boni et al., 2012). The systematic investigation of the impact of seroconversion on HBV-specific CD8⁺ T cell responses at the single-cell level reported here suggests instead that improved virus-specific T cell responses in chronically infected patients might precede, and possibly induce, HBsAg loss. Mechanistically, this may include the capacity of HBV-specific CD8⁺ T cells to reduce the levels of circulating HBsAg by killing or curing hepatocytes that produce HBsAg from episomal and/or integrated transcriptional templates. Whether circulating HBs clearance improves the response to subsequent therapeutic vaccination, as suggested by other investigators (Zhu et al., 2016), was not addressed in this study.

Whereas the current study evaluated the impact of circulating HBsAg on HBV-specific CD8⁺ T cell responses, previous work found that reducing the number of antigen-expressing hepatocytes (to <5%) or the amount of antigen per hepatocyte (by >15-fold) lowered HBV-specific CD8⁺ T cell expansion but was not sufficient per se to alter their propensity to evolve into dysfunctional cells lacking antiviral effector function (Bénéchet et al., 2019). Other studies have suggested that reducing hepatocellular antigen expression might increase the efficacy of

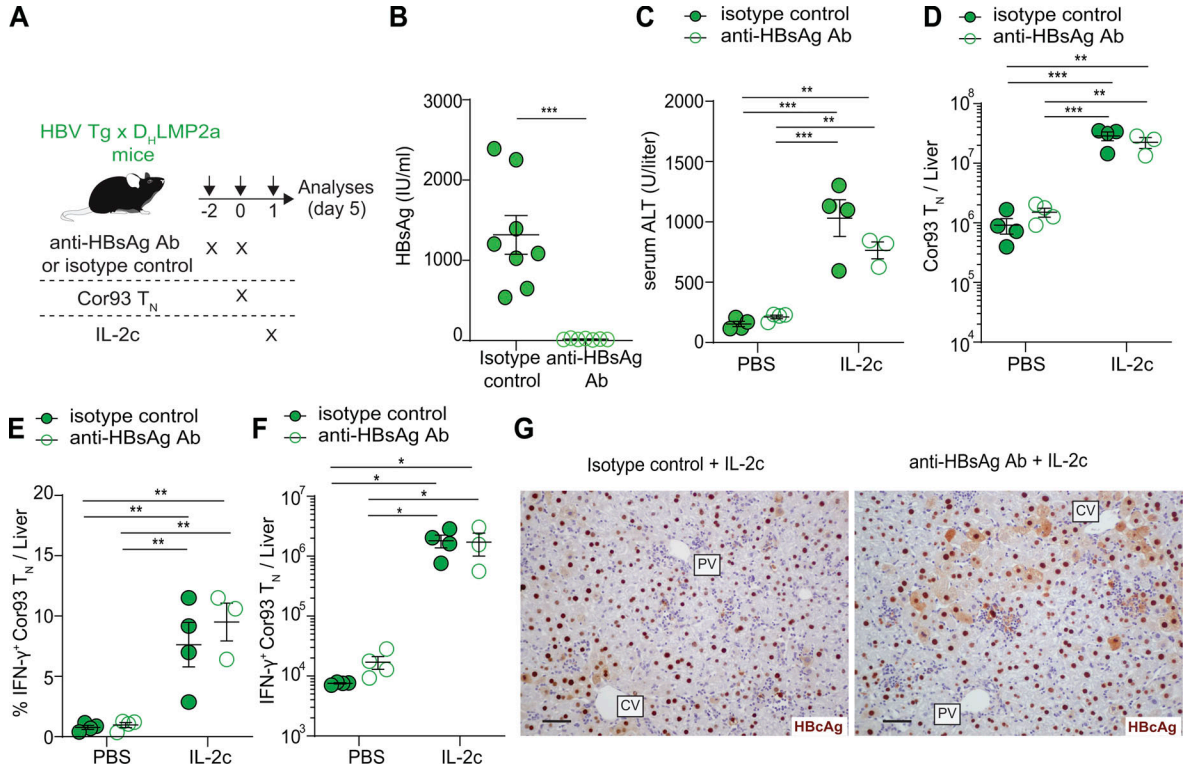

Figure 5. **Circulating HBsAg does not affect the functional improvement of intrahepatically primed CD8⁺ T cells by IL-2–based immunotherapeutic strategies. (A)** Schematic representation of the experimental setup (mouse drawings were adapted from Bénéchet et al., 2019). HBV Tg × D$_H$LMP2a mice were injected with HBsAb (empty symbols, *n* = 7) or isotype control (solid symbols, *n* = 8) before receiving 10^6 HBcAg-specific naive CD8⁺ T cells (Cor93 T$_N$) followed, 24 h later, by IL-2c (*n* = 7) or PBS (*n* = 8). Livers were collected and analyzed 5 d after Cor93 T$_N$ transfer. **(B)** Serum HBsAg concentrations (IU/ml) in mice injected with isotype control or HBsAb 1 d before Cor93 T$_N$ transfer. **(C)** Serum transaminase activity (ALT, U/liter) measured in the indicated mice 5 d after T cell transfer. **(D–F)** Absolute number of total Cor93 T cells (D), percentage (E), and absolute number (F) of IFN-γ–producing Cor93 T cells in the livers of the indicated mice 5 d after T cell transfer. **(G)** Representative immunohistochemical micrographs of liver sections 5 d after Cor93 T$_N$ injection from IL-2c–treated mice injected with isotype control (left) or HBsAb (right). HBcAg expression is shown in brown. Scale bars, 20 µm. CV, central vein; PV, portal vein. Data are expressed as mean ± SEM. Results are representative of two independent experiments. *, P < 0.05, **, P < 0.01, ***, P < 0.001; two-way ANOVA followed by Sidak's multiple comparison test (B–F). Comparisons are not statistically significant unless indicated.

subsequent therapeutic vaccination (Cobleigh et al., 2013; Michler et al., 2020).

A potential limitation of our study is that it relied on the adoptive transfer of a relatively large number of TCR transgenic CD8+ T cells. Since this is different from the polyclonal T cell response observed in chronically infected patients, it may raise issues related to the relevance of our findings. However, it is worth noting that endogenous HBV-specific CD8+ T cells are not deleted in the thymus of HBV transgenic mice; rather they are present in the periphery of adult mice; they are functionally silent and can be expanded and activated by, e.g., dendritic cell immunization (Shimizu et al., 1998), possibly reflecting the situation observed in chronically infected patients. Thus, the observation that HBsAg loss did not induce spontaneous immunopathology argues for HBsAg clearance per se not causing overt reactivation of HBV-specific tolerant T cells.

We believe that our results have significant clinical implications as monoclonal Abs against HBsAg are being evaluated for the treatment of chronic hepatitis B virus infection (Li et al., 2017; Zhang et al., 2016; Neumann et al., 2010; Galun et al., 2002). While treatment of chronically infected patients with monoclonal Abs targeting HBsAg might have the benefit of reducing the covalently closed circular DNA pool maintained by infection of new hepatocytes (Fanning et al., 2019), a potentially important aspect that we could not assess as mouse hepatocytes are refractory to HBV infection, the data presented here suggest that, in contrast to other chronic viral infections such as the one caused by HIV (Niessl et al., 2020), anti-HBV Ab therapy alone is unlikely to increase virus-specific CD8+ T cell immunity.

Materials and methods

Mice

C57BL/6, CD45.1 (inbred C57BL/6), Balb/c, Thy1.1 (CBy.PL(B6)-*Thy*^{a}/ScrJ) mice were purchased from Charles River or The Jackson Laboratory. D_HLMP2A mice (Casola et al., 2004), which are devoid of surface-expressed and secreted Abs, were originally provided by K. Rajewsky (Harvard Medical School, Boston, MA) and bred >10 generations against C57BL/6 mice. HBV replication-competent transgenic mice (HBV Tg, lineage 1.3.32, inbred C57BL/6, H-2^b), which express all of the HBV antigens and replicate HBV in the liver at high levels without any evidence of cytopathology, have been previously described (Guidotti et al., 1995). In indicated experiments, HBV Tg mice were used as C57BL/6 × Balb/c (H-2^{bxd}) F1 hybrids or bred with D_HLMP2a mice. Cor93 TCR transgenic mice (lineage BC10.3, inbred CD45.1), in which >98% of the splenic CD8+ T cells recognize a K^b-restricted epitope located between residues 93 and 100 in the HBV core protein (MGLKFRQL), have been previously described (Isogawa et al., 2013). Env28 TCR transgenic mice (lineage 6C2.36, inbred Balb/c), in which ∼83% of the splenic CD8+ T cells recognize a L^d-restricted epitope located between residues 28 and 39 of HBsAg (IPQSLDSWWTSL), have been previously described (Isogawa et al., 2013). They were mated once with Thy1.1 mice (inbred Balb/c), so that the TCR transgenic T cells could be easily followed upon adoptive transfer by anti-Thy1.1 Ab staining. Mice were housed under specific pathogen-free conditions and used at 8 wk of age, unless otherwise indicated. In all experiments, mice were matched for age, sex, and (for the HBV Tg mice) serum HBeAg levels before experimental manipulations. All experimental animal procedures were approved by the Institutional Animal Committee of the San Raffaele Scientific Institute.

Naive CD8+ T cell isolation, effector CD8+ T cell differentiation, and adoptive transfer

Mice were adoptively transferred with 2.5 × 10^6 HBV-specific naive CD8+ TCR transgenic T cells isolated from the spleens of Cor93 and/or Env28 TCR transgenic mice, as previously described (Bénéchet et al., 2019). In indicated experiments, naive CD8+ T cells from the spleens of Cor93 or Env28 TCR transgenic mice were differentiated in vitro for 7–9 d into effector cells before adoptive transfer (10^7 effector cells per mouse), as described (Guidotti et al., 2015; Manjunath et al., 2001).

In vivo treatments

HBV Tg mice were injected intraperitoneally with 25 mg/kg of HBsAb (mouse IgG2a, GS650225 XTL-17; Eren et al., 2000) or isotype control Abs (mouse IgG2a, GS-652025 CRL-2185) 15, 12, 8, 5, and 1 d before HBV-specific naive CD8+ T cell transfer (in the experiments described in Fig. 4 I) or 2 d and 4 h before T cell transfer (in the experiments described in Fig. 5 A). In selected experiments, mice were injected intraperitoneally with IL-2c 1 d after HBV-specific naive CD8+ T cell transfer, as described (Bénéchet et al., 2019). IL-2c were prepared by mixing 1.5 µg of recombinant IL-2 (clone 402 ML/CF, R&D) with 50 µg anti–IL-2 monoclonal Ab (clone S4B6-1, BioXcell) per mouse, as previously described (Bénéchet et al., 2019; Boyman et al., 2006).

Cell isolation and flow cytometry

Single-cell suspensions of livers were generated as described (Bénéchet et al., 2019). For analysis of ex vivo intracellular cytokine production, single-cell suspensions of livers were obtained as described above except that 1 µg/ml of brefeldin A (Sigma-Aldrich) was included in the digestion buffer. All flow cytometry stainings of surface-expressed and intracellular molecules were performed as described (Bénéchet et al., 2019). Cell viability was assessed by staining with Viobility 405/520 fixable dye (130-109-814, Miltenyi). Abs used included anti-CD8 (clone: 53–6.7, 558106, BD Biosciences), anti-CD45.1 (clone: A20, 110708, 110720, 110718, BD Biosciences), anti-CD90.1 (clone: OX-7, 561404, BD Biosciences), anti-CD25 (clone: PC61, 102017), anti-CD69 (clone: H1.2F3, 552879, BD Biosciences; 104525), anti-LAG-3 (clone: C9B7W, 125212), anti-PD-1 (clone: J43, 17-9985, 17-9985, eBioscience), anti-CD62-L (clone: MEL-14, 104428, 104420), anti-CD44 (clone: IM7, 103032, 103027), anti-IFN-γ (clone: XMG1.2, 557735 BD Biosciences; 505813), and anti-Granzyme B (clone: GB11, 515406; clone: QA16A02, 372207). All Abs were purchased from BioLegend, unless otherwise indicated. Recombinant dimeric H-2L^d:Ig and H-2K^b:Ig fusion proteins (BD Biosciences) complexed with peptides derived from HBsAg (Env28-39) or from HBcAg (Cor93-100), respectively, were prepared according to the manufacturer's instructions. Dimer staining was performed as described (Iannacone et al., 2005).

All flow cytometry analyses were performed in FACS buffer containing PBS with 2 mM EDTA and 2% FBS on a FACS CANTO II (Becton Dickinson) and analyzed with FlowJo software (Treestar).

Purification of viral nucleic acids from serum and quantitative PCR (qPCR) analyses

To isolate viral nucleic acids, 20 µl of serum were incubated for 2 h at 37°C with 180 µl IsoHi Buffer (150 mM NaCl, 0.5% NP-40, 10 mM Tris, pH 7.4), 5 mM $CaCl_2$, 5 mM $MgCl_2$, 1 U DNaseI (Life Technologies, AM1907), and 5 U Micrococcal Nuclease (New England Biolabs, MO247S). The digestion was stopped by the addition of 20 mM EDTA, pH 8.0, and viral nucleic acid purification performed with the QIAmp MiniElute Virus Spin Kit (Qiagen, 57704), according to the manufacturer's instructions.

DNA

Serum nucleic acids were diluted 100 times, and qPCR was performed using TaqMan Fast Universal PCR Master Mix (Life Technologies, 4352042).

RNA

DNA was removed from purified serum nucleic acid using Ambion 10 TURBO DNA-freeTM DNase (AM1907). Total RNA was reverse-transcribed and amplified using TaqMan Fast Virus 1-Step PCR Master Mix (Life Technologies, 4444464).

Viremia quantification was performed for HBV envelope (forward: 5′-CCCGTTTGTCCTCTAATTCC-3′; reverse: 5′-GTC CGAAGGTTTGGTACAGC-3′; probe: 5′-CTCAACAACCAGCAC GGGACCA-3′) by absolute qPCR using a standard curve drawn with plasmid DNA. Reactions were run and analyzed on Quant Studio 5 instrument (Life Technologies). All experiments were performed in duplicate.

Purification and analysis of viral RNA from liver

RNA was extracted from frozen livers (left lobe) using ReliaPrep RNA Tissue Miniprep System (Promega, Z6111), according to the manufacturer's instructions, and genomic DNA was removed using Ambion TURBO DNA-freeTM DNase (AM1907). DNA lysis was performed with 5 µg of extracted RNA. 200 ng of total RNA was reverse-transcribed with Superscript IV Vilo (Life Technologies, 11766050) before qPCR analysis for HBV envelope. Reactions were run and analyzed on Quant Studio 5 instrument (Life Technologies). Analysis were normalized to the reference gene *Gapdh* (Life Technologies, Mm99999915_g1). All experiments were performed in duplicate.

Liver DNA isolation and Southern blot analysis

Total liver DNA was analyzed for HBV replicative intermediates by Southern blot analysis, as described (Guidotti et al., 1996). Nylon transfer membranes (Roche, 11417240001) were hybridized with a digoxigenin-labeled HBV DNA probe (DIG High Prime DNA Labeling and Detection Starter kit II, Roche, 115856149109), according to the manufacturer's instructions. Image acquisition was obtained after 24 h membrane exposure on a Syngene Imaging System.

Histochemistry

For H&E staining and HBcAg immunohistochemistry, livers were perfused with PBS, harvested in Zn-formalin, and transferred into 70% ethanol 24 h later. Tissues were then processed, embedded in paraffin, and stained as previously described (Guidotti et al., 2015). Bright-field images were acquired through an Aperio Scanscope System CS2 microscope and an ImageScope program (Leica Biosystem) following the manufacturer's instructions.

Biochemical analyses

Serum HBsAg, HBeAg, and HBsAb were measured by ELISA, as previously described (Bénéchet et al., 2019; Tonti et al., 2013). The extent of hepatocellular injury was monitored by measuring plasma alanine aminotransferase (ALT) activity at multiple time points after treatment, as previously described (Guidotti et al., 2015).

Statistical analyses

Results are expressed as mean ± SEM. All statistical analyses were performed in Prism (GraphPad Software, version 8). Means between two groups were compared with the Mann–Whitney *U* test. Means among three or more groups were compared with two-way ANOVA followed by Sidak's multiple comparison test. Kaplan–Meier curves were compared with the log-rank (Mantel–Cox) test. Comparisons are not statistically significant unless indicated.

Online supplemental material

Fig. S1 shows no correlation between early serum transaminases or viremia and subsequent serum HBsAg loss; moreover, it shows that HBsAg loss in HBV Tg mice is not due to decreased hepatic expression or to increased hepatocellular retention. Fig. S2 describes the phenotype and antiviral activity of adoptively transferred HBV-specific effector $CD8^+$ T cells in the liver of $HBsAg^+$ and $HBsAg^-$ HBV Tg mice. Fig. S3 depicts the phenotype and function of adoptively transferred HBV-specific naive $CD8^+$ T cells in the liver of $HBsAg^+$ and $HBsAg^-$ HBV Tg mice.

Acknowledgments

We thank M. Mainetti, M. Freschi, M. Raso, and A. Fiocchi for technical support; M. Silva for secretarial assistance; and the members of the Iannacone laboratory for helpful discussions. Flow cytometry was carried out at FRACTAL, a flow cytometry resource and advanced cytometry technical applications laboratory established by the San Raffaele Scientific Institute. We would like to acknowledge the PhD program in Basic and Applied Immunology and Oncology at Vita-Salute San Raffaele University, as V. Fumagalli and V. Venzin conducted this study as partial fulfillment of their PhDs in Molecular Medicine within that program.

M. Iannacone is supported by European Research Council consolidator grants 725038 and 957502, Italian Association for Cancer Research grants 19891 and 22737, Italian Ministry of Health grant RF-2018-12365801, Lombardy Foundation for Biomedical Research grant 2015-0010, the European Molecular Biology Organization Young Investigator Program, and a Funded Research Agreement from Gilead Sciences. L.G. Guidotti is supported by Italian Association for Cancer Research grant 22737, Lombardy Open Innovation grant 229452, Italian

Ministry of Education, University and Research Progetto di ricerca di Rilevante Interesse Nazionale (PRIN) grant 2017MPCWPY, and a Funded Research Agreement from Gilead Sciences.

Author contributions: V. Fumagalli designed and performed experiments, analyzed data, performed the statistical analyses, prepared the figures, and drafted the manuscript; P. Di Lucia, V. Venzin, and E.B. Bono performed experiments and analyzed data; R. Jordan, C.R. Frey, and W. Delaney provided and characterized the monoclonal Ab targeting HBsAg; F.V. Chisari provided conceptual advice and edited the manuscript; L.G. Guidotti provided funding and conceptual advice and edited the manuscript; M. Iannacone designed and coordinated the study, provided funding, and wrote the paper.

Disclosures: R. Jordan reported personal fees from Gilead Sciences during the conduct of the study and outside the submitted work, and is a shareholder of Gilead Sciences. C.R. Frey reported personal fees from Gilead Sciences during the conduct of the study. F.V. Chisari reported personal fees from Gilead Sciences, Vir Biotechnology, and Avalia Immunotherapies outside the submitted work. L.G. Guidotti reported grants and personal fees from Gilead Sciences during the conduct of the study. M. Iannacone reported grants from Gilead Sciences during the conduct of the study and personal fees from Gilead Sciences outside the submitted work. No other disclosures were reported.

Submitted: 19 February 2020
Revised: 20 April 2020
Accepted: 18 June 2020

References

Bazinet, M., V. Pântea, G. Placinta, I. Moscalu, V. Cebotarescu, L. Cojuhari, P. Jimbei, L. Iarovoi, V. Smesnoi, T. Musteata, et al. 2020. Safety and Efficacy of 48 Weeks REP 2139 or REP 2165, Tenofovir Disoproxil, and Pegylated Interferon Alfa-2a in Patients With Chronic HBV Infection Naïve to Nucleos(t)ide Therapy. *Gastroenterology*. 158:2180–2194. https://doi.org/10.1053/j.gastro.2020.02.058

Bénéchet, A.P., G. De Simone, P. Di Lucia, F. Cilenti, G. Barbiera, N. Le Bert, V. Fumagalli, E. Lusito, F. Moalli, V. Bianchessi, et al. 2019. Dynamics and genomic landscape of CD8$^+$ T cells undergoing hepatic priming. *Nature*. 574:200–205. https://doi.org/10.1038/s41586-019-1620-6

Boni, C., D. Laccabue, P. Lampertico, T. Giuberti, M. Viganò, S. Schivazappa, A. Alfieri, M. Pesci, G.B. Gaeta, G. Brancaccio, et al. 2012. Restored function of HBV-specific T cells after long-term effective therapy with nucleos(t)ide analogues. *Gastroenterology*. 143:963–73.e9. https://doi.org/10.1053/j.gastro.2012.07.014

Boyman, O., M. Kovar, M.P. Rubinstein, C.D. Surh, and J. Sprent. 2006. Selective stimulation of T cell subsets with antibody-cytokine immune complexes. *Science*. 311:1924–1927. https://doi.org/10.1126/science.1122927

Casola, S., K.L. Otipoby, M. Alimzhanov, S. Humme, N. Uyttersprot, J.L. Kutok, M.C. Carroll, and K. Rajewsky. 2004. B cell receptor signal strength determines B cell fate. *Nat. Immunol.* 5:317–327. https://doi.org/10.1038/ni1036

Cobleigh, M.A., X. Wei, and M.D. Robek. 2013. A vesicular stomatitis virus-based therapeutic vaccine generates a functional CD8 T cell response to hepatitis B virus in transgenic mice. *J. Virol.* 87:2969–2973. https://doi.org/10.1128/JVI.02111-12

de Niet, A., L. Jansen, H.L. Zaaijer, U. Klause, B. Takkenberg, H.L.A. Janssen, T. Chu, R. Petric, and H.W. Reesink. 2014. Experimental HBsAg/anti-HBs complex assay for prediction of HBeAg loss in chronic hepatitis B patients treated with pegylated interferon and adefovir. *Antivir. Ther. (Lond.)*. 19:259–267. https://doi.org/10.3851/IMP2707

Eren, R., E. Ilan, O. Nussbaum, I. Lubin, D. Terkieltaub, Y. Arazi, O. Ben-Moshe, A. Kitchinzky, S. Berr, J. Gopher, et al. 2000. Preclinical evaluation of two human anti-hepatitis B virus (HBV) monoclonal antibodies in the HBV-trimera mouse model and in HBV chronic carrier chimpanzees. *Hepatology*. 32:588–596. https://doi.org/10.1053/jhep.2000.9632

Fanning, G.C., F. Zoulim, J. Hou, and A. Bertoletti. 2019. Therapeutic strategies for hepatitis B virus infection: towards a cure. *Nat. Rev. Drug Discov.* 18:827–844. https://doi.org/10.1038/s41573-019-0037-0

Galun, E., R. Eren, R. Safadi, Y. Ashour, N. Terrault, E.B. Keeffe, E. Matot, S. Mizrachi, D. Terkieltaub, M. Zohar, et al. 2002. Clinical evaluation (phase I) of a combination of two human monoclonal antibodies to HBV: safety and antiviral properties. *Hepatology*. 35:673–679. https://doi.org/10.1053/jhep.2002.31867

Guidotti, L.G., and F.V. Chisari. 2006. Immunobiology and pathogenesis of viral hepatitis. *Annu. Rev. Pathol.* 1:23–61. https://doi.org/10.1146/annurev.pathol.1.110304.100230

Guidotti, L.G., B. Matzke, H. Schaller, and F.V. Chisari. 1995. High-level hepatitis B virus replication in transgenic mice. *J. Virol.* 69:6158–6169. https://doi.org/10.1128/JVI.69.10.6158-6169.1995

Guidotti, L.G., T. Ishikawa, M.V. Hobbs, B. Matzke, R. Schreiber, and F.V. Chisari. 1996. Intracellular inactivation of the hepatitis B virus by cytotoxic T lymphocytes. *Immunity*. 4:25–36. https://doi.org/10.1016/S1074-7613(00)80295-2

Guidotti, L.G., D. Inverso, L. Sironi, P. Di Lucia, J. Fioravanti, L. Ganzer, A. Fiocchi, M. Vacca, R. Aiolfi, S. Sammicheli, et al. 2015. Immunosurveillance of the liver by intravascular effector CD8(+) T cells. *Cell*. 161:486–500. https://doi.org/10.1016/j.cell.2015.03.005

Iannacone, M., G. Sitia, M. Isogawa, P. Marchese, M.G. Castro, P.R. Lowenstein, F.V. Chisari, Z.M. Ruggeri, and L.G. Guidotti. 2005. Platelets mediate cytotoxic T lymphocyte-induced liver damage. *Nat. Med.* 11:1167–1169. https://doi.org/10.1038/nm1317

Isogawa, M., J. Chung, Y. Murata, K. Kakimi, and F.V. Chisari. 2013. CD40 activation rescues antiviral CD8$^+$ T cells from PD-1-mediated exhaustion. *PLoS Pathog.* 9. e1003490. https://doi.org/10.1371/journal.ppat.1003490

Kim, C.Y., and J.G. Tilles. 1973. Purification and biophysical characterization of hepatitis B antigen. *J. Clin. Invest.* 52:1176–1186. https://doi.org/10.1172/JCI107284

Li, D., W. He, X. Liu, S. Zheng, Y. Qi, H. Li, F. Mao, J. Liu, Y. Sun, L. Pan, et al. 2017. A potent human neutralizing antibody Fc-dependently reduces established HBV infections. *eLife*. 6. e26738. https://doi.org/10.7554/eLife.26738

Liaw, Y.-F. 2019. Clinical utility of HBV surface antigen quantification in HBV e antigen-negative chronic HBV infection. *Nat. Rev. Gastroenterol. Hepatol.* 16:631–641. https://doi.org/10.1038/s41575-019-0197-8

Manjunath, N., P. Shankar, J. Wan, W. Weninger, M.A. Crowley, K. Hieshima, T.A. Springer, X. Fan, H. Shen, J. Lieberman, et al. 2001. Effector differentiation is not prerequisite for generation of memory cytotoxic T lymphocytes. *J. Clin. Invest.* 108:871–878. https://doi.org/10.1172/JCI13296

Michler, T., A.D. Kosinska, J. Festag, T. Bunse, J. Su, M. Ringelhan, H. Imhof, D. Grimm, K. Steiger, C. Mogler, et al. 2020. Knockdown of Virus Antigen Expression Increases Therapeutic Vaccine Efficacy in High-Titer Hepatitis B Virus Carrier Mice. *Gastroenterology*. 158:1762–1775.e9. https://doi.org/10.1053/j.gastro.2020.01.032

Neumann, A.U., S. Phillips, I. Levine, S. Ijaz, H. Dahari, R. Eren, S. Dagan, and N.V. Naoumov. 2010. Novel mechanism of antibodies to hepatitis B virus in blocking viral particle release from cells. *Hepatology*. 52:875–885. https://doi.org/10.1002/hep.23778

Niessl, J., A.E. Baxter, P. Mendoza, M. Jankovic, Y.Z. Cohen, A.L. Butler, C.-L. Lu, M. Dubé, I. Shimeliovich, H. Gruell, et al. 2020. Combination anti-HIV-1 antibody therapy is associated with increased virus-specific T cell immunity. *Nat. Med.* 26:222–227. https://doi.org/10.1038/s41591-019-0747-1

Seeger, C., and W.S. Mason. 2015. Molecular biology of hepatitis B virus infection. *Virology*. 479-480:672–686. https://doi.org/10.1016/j.virol.2015.02.031

Shimizu, Y., L.G. Guidotti, P. Fowler, and F.V. Chisari. 1998. Dendritic cell immunization breaks cytotoxic T lymphocyte tolerance in hepatitis B virus transgenic mice. *J. Immunol.* 161:4520–4529.

Sitia, G., R. Aiolfi, P. Di Lucia, M. Mainetti, A. Fiocchi, F. Mingozzi, A. Esposito, Z.M. Ruggeri, F.V. Chisari, M. Iannacone, et al. 2012. Antiplatelet therapy prevents hepatocellular carcinoma and improves survival in a mouse model of chronic hepatitis B. *Proc. Natl. Acad. Sci. USA*. 109:E2165–E2172. https://doi.org/10.1073/pnas.1209182109

Tonti, E., N. Jiménez de Oya, G. Galliverti, E.A. Moseman, P. Di Lucia, A. Amabile, S. Sammicheli, M. De Giovanni, L. Sironi, N. Chevrier, et al. 2013. Bisphosphonates target B cells to enhance humoral immune responses. *Cell Rep*. 5:323–330. https://doi.org/10.1016/j.celrep.2013.09.004

Wooddell, C.I., M.-F. Yuen, H.L.-Y. Chan, R.G. Gish, S.A. Locarnini, D. Chavez, C. Ferrari, B.D. Given, J. Hamilton, S.B. Kanner, et al. 2017. RNAi-based treatment of chronically infected patients and chimpanzees reveals that integrated hepatitis B virus DNA is a source of HBsAg. *Sci. Transl. Med*. 9. eaan0241. https://doi.org/10.1126/scitranslmed.aan0241

Zhang, T.-Y., Q. Yuan, J.-H. Zhao, Y.-L. Zhang, L.-Z. Yuan, Y. Lan, Y.-C. Lo, C.-P. Sun, C.-R. Wu, J.-F. Zhang, et al. 2016. Prolonged suppression of HBV in mice by a novel antibody that targets a unique epitope on hepatitis B surface antigen. *Gut*. 65:658–671. https://doi.org/10.1136/gutjnl-2014-308964

Zhu, D., L. Liu, D. Yang, S. Fu, Y. Bian, Z. Sun, J. He, L. Su, L. Zhang, H. Peng, et al. 2016. Clearing Persistent Extracellular Antigen of Hepatitis B Virus: An Immunomodulatory Strategy To Reverse Tolerance for an Effective Therapeutic Vaccination. *J. Immunol*. 196:3079–3087. https://doi.org/10.4049/jimmunol.1502061

Supplemental material

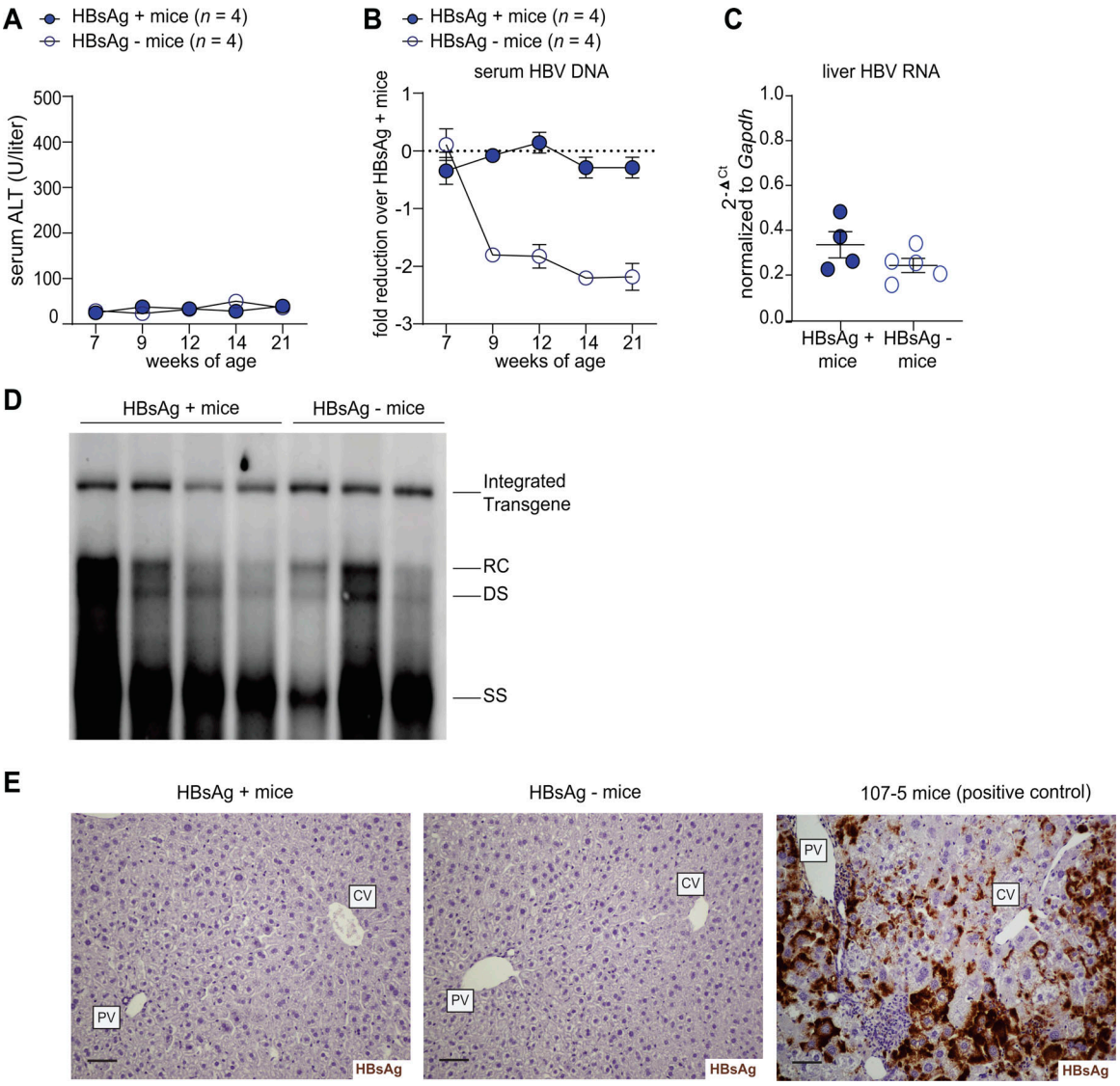

Figure S1. **HBsAg loss in HBV Tg mice is not due to decreased hepatic expression nor to increased hepatocellular retention. (A and B)** Serum transaminase activity (ALT, U/liter; A) and serum HBV DNA quantification (B) in $HBsAg^+$ (solid blue symbols, $n = 4$), $HBsAg^-$ (empty blue symbols, $n = 4$) HBV Tg mice measured at 7, 9, 12, 14, and 21 wk of age. HBV DNA values are expressed as fold reduction over Ab-competent $HBsAg^+$ HBV Tg mice. **(C)** Quantification of HBV RNA in the liver of $HBsAg^+$ (solid symbols, $n = 4$) and $HBsAg^-$ (empty symbols, $n = 5$) HBV Tg mice. Values were normalized to the reference gene *Gapdh*. **(D)** HBV DNA quantification by Southern blot analysis in the liver of $HBsAg^+$ ($n = 4$) and $HBsAg^-$ ($n = 3$) HBV Tg mice. Bands corresponding to the expected size of the integrated transgene, relaxed circular (RC), double-stranded linear (DS), and single-stranded (SS) HBV DNAs are indicated. **(E)** Representative immunohistochemical micrographs of liver sections from $HBsAg^+$ (left) and $HBsAg^-$ (middle) HBV Tg mice. HBsAg expression is shown in brown. An immunohistochemical micrograph of a liver section from a positive control (107–5 mouse undergoing immune-mediated chronic hepatitis; Sitia et al., 2012) is shown at the right. Scale bars, 20 µm. CV, central vein; PV, portal vein. Data are expressed as mean ± SEM. Two-way ANOVA followed by Sidak's multiple comparison test (A); Mann–Whitney *U* test (C). Comparisons are not statistically significant unless indicated.

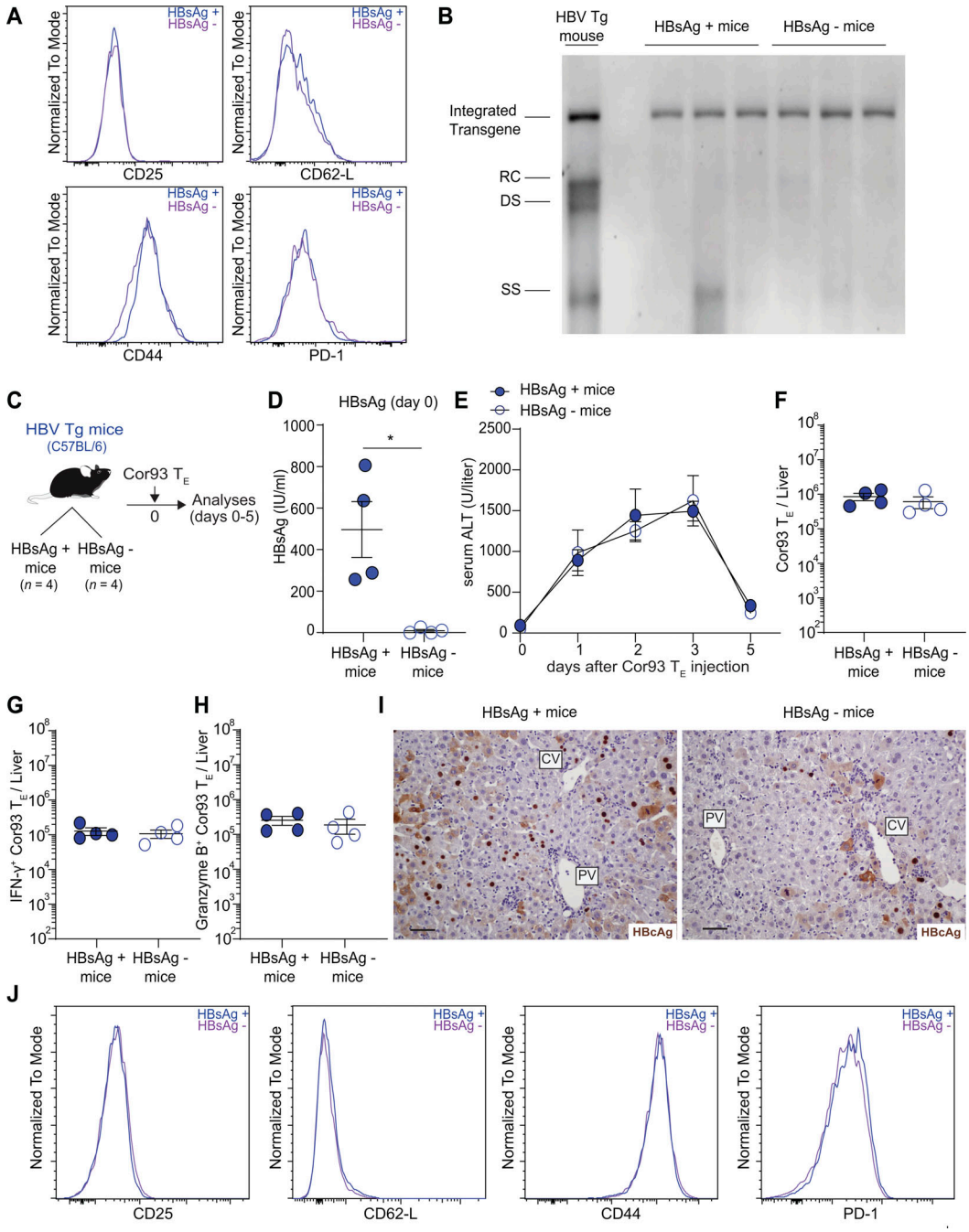

Figure S2. **Clearance of circulating HBsAg has no impact on the phenotype and function of intrahepatic HBV-specific effector CD8⁺ T cells.** **(A)** Representative flow cytometry histograms showing the mean fluorescent intensity (MFI) of CD25, CD62-L, CD44, and PD-1 expression by Env28 T_E (gated as CD8⁺ Thy1.1⁺ live cells) isolated from the liver of HBsAg⁺ (blue) and HBsAg⁻ (purple) HBV Tg mice 5 d after T cell transfer. **(B)** HBV DNA quantification by Southern blot analysis in the liver of HBsAg⁺ (n = 3) and HBsAg⁻ (n = 3) HBV Tg mice 5 d after Env28 T_E adoptive transfer. Pool of HBV DNA extracted from the liver of HBV Tg mice as control. Bands corresponding to the expected size of the integrated transgene, relaxed circular (RC), double-stranded linear (DS), and single-stranded (SS) HBV DNAs are indicated. **(C)** Schematic representation of the experimental setup (mouse drawings were adapted from Bénéchet et al., 2019). HBsAg⁺ (solid symbols, n = 4) and HBsAg⁻ HBV Tg mice (empty symbols, n = 4) received 10^7 HBcAg-specific effector CD8⁺ T cells (Cor93 T_E). Livers were collected and analyzed 5 d after Cor93 T_E transfer. Serum was collected immediately before and 1, 2, 3, and 5 d after Cor93 T_E transfer. **(D)** Serum HBsAg concentrations (IU/ml) in HBsAg⁺ and HBsAg⁻ HBV Tg mice before Cor93 T_E injection. **(E)** Serum transaminase activity (ALT, U/liter) in HBsAg⁺ and HBsAg⁻ HBV Tg mice after Cor93 T_E injection. **(F–H)** Absolute number of (F) total Cor93 T_E and absolute number of (G) IFN-γ– and (H) granzyme B–producing Cor93 T_E cells in the livers of HBsAg⁺ and HBsAg⁻ HBV Tg mice 5 d after Cor93 T_E injection. **(I)** Representative immunohistochemical micrographs of liver sections from HBsAg⁺ (left) and HBsAg⁻ (right) HBV Tg mice 5 d after Cor93 T_E injection. HBcAg expression is shown in brown. Scale bars, 20 µm. CV, central vein; PV, portal vein. **(J)** Representative flow cytometry histograms show the MFI of CD25, CD62-L, CD44, and PD-1 expression by Cor93 T_E cells (gated as CD8⁺ CD45.1⁺ live cells) isolated from the liver of HBsAg⁺ (blue) and HBsAg⁻ (purple) HBV Tg mice 5 d after T cell transfer. Data are expressed as mean ± SEM. Results are representative of two independent experiments. *, P < 0.05; Mann-Whitney U test (D and F–H), two-way ANOVA followed by Sidak's multiple comparison test (E). Comparisons are not statistically significant unless indicated.

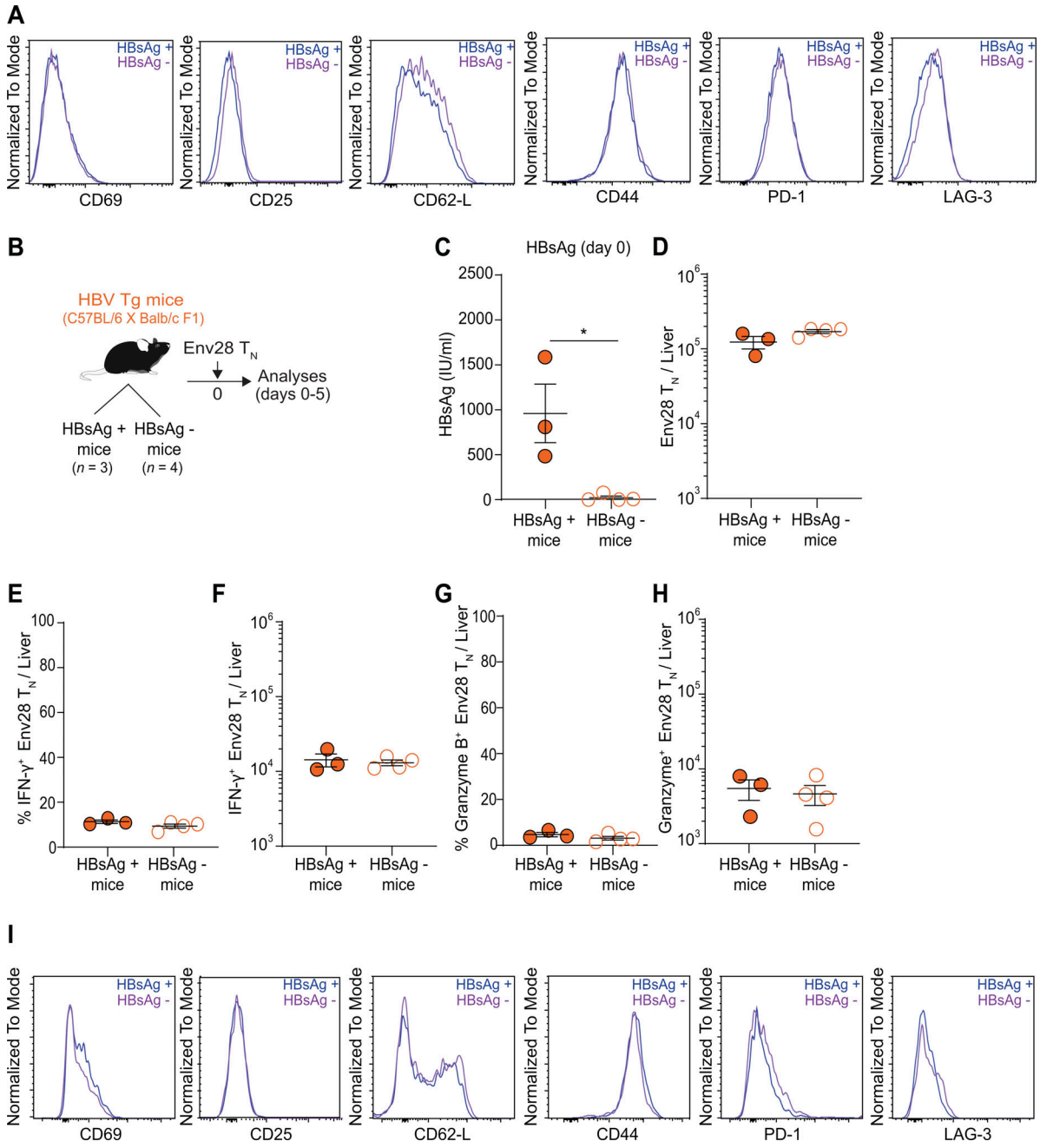

Figure S3. **Clearance of circulating HBsAg has no impact on the phenotype and differentiation of HBV-specific naive CD8⁺ T cells into dysfunctional cells upon hepatocellular priming. (A)** Representative flow cytometry histograms showing the MFI of CD69, CD25, CD62-L, CD44, PD-1, and LAG-3 expression by Cor93 T cells (gated as CD8⁺ CD45.1⁺ live cells) isolated from the liver of HBsAg⁺ (blue) and HBsAg⁻ (purple) HBV Tg mice 5 d after adoptive cell transfer. **(B)** Schematic representation of the experimental setup (mouse drawings were adapted from Bénéchet et al., 2019). HBsAg⁺ (solid symbols, *n* = 3) and HBsAg⁻ (empty symbols, *n* = 4) HBV Tg mice (on a C57BL/6 × Balb/c F1 hybrid background) received 2.5 × 10^6 HBsAg-specific naive CD8⁺ T cells (Env28 T_N). Livers were collected and analyzed 5 d after Env28 T_N transfer. Serum was collected immediately before and 5 d after Env28 T_N transfer. **(C)** HBsAg concentrations (IU/ml) in the serum of HBsAg⁺ and HBsAg⁻ HBV Tg mice before Env28 T_N injection. **(D)** Absolute number of total Env28 T_N in the livers of HBsAg⁺ and HBsAg⁻ HBV Tg mice 5 d after Env28 T_N injection. **(E–H)** Percentage (E and G) and absolute number (F and H) of IFN-γ⁺ (E and F) and Granzyme B⁺ (G and H) Env28 T_N cells in the livers of HBsAg⁺ and HBsAg⁻ HBV Tg mice 5 d after Env28 T_N injection. **(I)** Representative flow cytometry histograms showing the MFI of CD69, CD25, CD62-L, CD44, PD-1, and LAG-3 expression by Env28 T cells (gated as CD8⁺ Thy1.1⁺ live cells) isolated from the liver of HBsAg⁺ (blue) and HBsAg⁻ (purple) HBV Tg mice 5 d after adoptive cell transfer. Data are expressed as mean ± SEM. Results are representative of two independent experiments. *, P < 0.05; Mann–Whitney *U* test (C–H). Comparisons are not statistically significant unless indicated.